Pramāṇa, Vol. 22, No. 5, May 1984, pp. 387–405. © Printed in India.

Phase transitions of a feedback amplifier

K NEELAKANTAN and G VENKATARAMAN
Reactor Research Centre, Kalpakkam 603 102, India

MS received 19 September 1983; revised 16 February 1984

Abstract. The phase transition behaviour of an amplifier with positive feedback is experimentally studied. The results are interpreted using catastrophe theory language. Zero (in Gilmore's classification), first and second-order transitions are demonstrated by driving the system along appropriate trajectories in control parameter space and the cusp and the spinodal are mapped. The fluctuations of the order parameter are investigated and their relationship to system response time established. Quench experiments analogous to those familiar in condensed matter have also been performed and with similar results.

Keywords. Nonequilibrium phase transitions; catastrophe theory; order parameter kinetics; feedback amplifier.

1. Introduction

It is now widely recognised that a system driven far from equilibrium can exhibit phenomena akin to the familiar equilibrium phase transitions (Glansdorf and Prigogine 1971; Haken 1978). Christened nonequilibrium phase transitions, such phenomena are seen in diverse fields—hydrodynamics (Swinney and Gollub 1981), electronics (Landauer 1962), optics (Haken 1978; Arecchi 1979), chemistry (Nicolis 1980; Pacault and Vidal 1979) and biology (Nicolis and Prigogine 1977), to name a few. It is even conjectured that nonequilibrium phase transition concepts might be relevant in the context of the origin of life (Eigen 1971; Prigogine and Nicolis 1971; Venkataraman and Balakrishnan 1978).

The analogy to equilibrium phase transitions is not confined to the manifestation of a new state alone. Indeed concepts like the order parameter, order-parameter fluctuations, symmetry breaking etc have also been carried over successfully (Haken 1978). Our own interest is in examples pertaining to metallurgy (Venkataraman 1979), and while performing some simulation experiments (Neelakantan and Venkataraman 1982) we noted that the feedback amplifier offered a convenient vehicle for exploring various concepts pertaining to nonequilibrium phase transitions. In this paper we report the results of our subsequent investigations regarding the phase transition aspects of such an amplifier. Electronics provides many examples, starting with the oft-quoted one of a public address system going into a howl. Theoretical and experimental results pertaining tc certain specific aspects like the existence of the transition and the growth of fluctuations are available for many systems. Examples include the tunnel diode (Landauer 1962), Josephson junction (Shenoy and Agarwal 1981), the Gunn diode (Haken 1978; Keizer 1981), Wien-bridge oscillator (Kawakubo and Kabashima 1974; Horn *et al* 1976), parametric amplifier (Kabashima *et al* 1979) etc. As compared to the papers cited above, our interest was to investigate various aspects by close analogy to condensed matter physics. It is also worth stressing that the experiments we report are of pedagogic value too and could easily form a part of the practicals in a Master's course, enabling students to study with ease various aspects of phase transitions. Indeed several extensions to our work are also possible as we will indicate towards the end.

The organization of this paper is as follows: In §2 we gather together some of the basic concepts (such as we need) relating to phase transitions. The language of catastrophe theory is extensively used, that being particularly convenient in the present case. The system investigated is described in §3 while the experiments performed and the results obtained are presented in §4. Concluding remarks are made at the end as usual.

2. Some relevant facts—A review

Let us suppose we start with a system initially not coupled to the outside and which is in a state of equilibrium. We now couple it to the external world suitably so that it can exchange energy and/or matter. A laser, for example, exchanges energy with the outside while a biosystem exchanges both energy and matter. Via the coupling introduced, we imagine a stationary external force to be applied to the system, the magnitude of the force being at our disposal. When the force is small, the response will be linear and, after the transients have died down, the system will settle down into a steady state. The succession of steady states that develop when the force is gradually increased from zero is often referred to as the thermodynamic branch. It frequently happens that when the system is driven farther and farther away from equilibrium, the steady state corresponding to the thermodynamic branch becomes unstable. At this stage, one or more totally new options become available to the system, some of which may be unstable while others may be stable. The system then crosses over from the thermodynamic branch to one of the newly available stable branches. This phenomenon is called bifurcation, a simple example of which is illustrated in figure 1.

Now the traditional approach to equilibrium phase transitions is *via* the Landau theory (Landau and Lifshitz 1959) where one starts with the free energy expansion

$$F = F_0 + (A/2)\psi^2 + (B/4)\psi^4. \tag{1}$$

Here ψ is the order parameter, and A and B are coefficients of which B is positive, while A varies with temperature as $\alpha_0(T-T_c)$. For $T > T_c$, the minimum of F occurs for $\psi = 0$ whereas for $T < T_c$, F has a double well structure leading to a nonzero value of ψ corresponding to the free energy minimum. The transition at T_c is second order. If an external field is applied, then a term $H\psi$ must be added to the right side of (1), H being the field (conjugate to ψ).

In nonequilibrium transitions, one does not always have a quantity analogous to F but fortunately, for the feedback amplifier there does exist a potential V which plays a similar role. Accordingly, we follow Gilmore (1981) and consider a potential of the form

$$V(x; a, b) = (a/2)x^2 + (x^4/4) + bx. \tag{2}$$

Here x is the order parameter, while a and b are the control parameters. The term bx describes the effects of the field. The space of (a, b) is the control parameter space. In the language of catastrophe theory (Gilmore 1981), (2) is the cusp catastrophe A_{+3}. As we

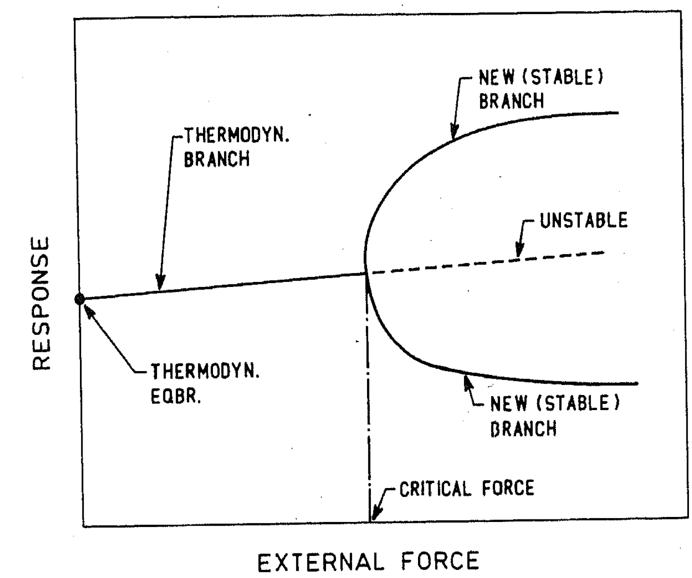

Figure 1. Schematic illustration of bifurcation. For explanation see text.

shall see later, the potential function for the feedback amplifier can be cast in the form (2).

Our interest is in the minima of V since they govern the steady state, and for this reason we focus attention on the critical manifold defined by $(\mathrm{d}V/\mathrm{d}x) = 0$. This manifold (figure 2), has a S-shaped fold. The projection of the fold lines on the a-b plane is given by (Gilmore 1981)

$$(a/3)^3 + (b/2)^2 = 0, \tag{3}$$

and is a cusp. When the system is maintained at conditions corresponding to any given point in control parameter space, it seeks that value of x for which V is a minimum. As the control parameters are varied *i.e.* when one traces a trajectory in the a-b plane, x evolves through a succession of appropriate minima and when multiple options are available it switches over to a new, more stable state. It is in the discussion of such a switch-over that the critical manifold is particularly useful. Presently we shall consider the system behaviour relating to a few important and representative trajectories. Incidentally, in contrast to equilibrium phase transitions where the usual control is the variation of T (equivalent of a in (2)), in the system we have studied, we have the facility to vary both a and b quite easily.

Consider first the trajectory marked ① in figure 3. Here $b = 0$ whence it corresponds to a field-free situation. On the right of figure 3 are sketched the forms of V appropriate to various points on the trajectory. As one can easily see, a bifurcation develops as the parameter a crosses from positive to negative values; the related transition is of second order. *Vis-a-vis* the critical manifold, the trajectory pierces it and rides on the central sheet of the S-shaped fold. However, this central sheet represents instability as it corresponds to a maximum of V; as a result, the system switches to either the top or the bottom fold (both of which represent stable states) and rides it thereafter. This behavioural pattern is better discussed using a 'surgered manifold' as we shall do later.

Next we consider trajectories ② and ③ in figure 3. Since $b \neq 0$, they do not pierce

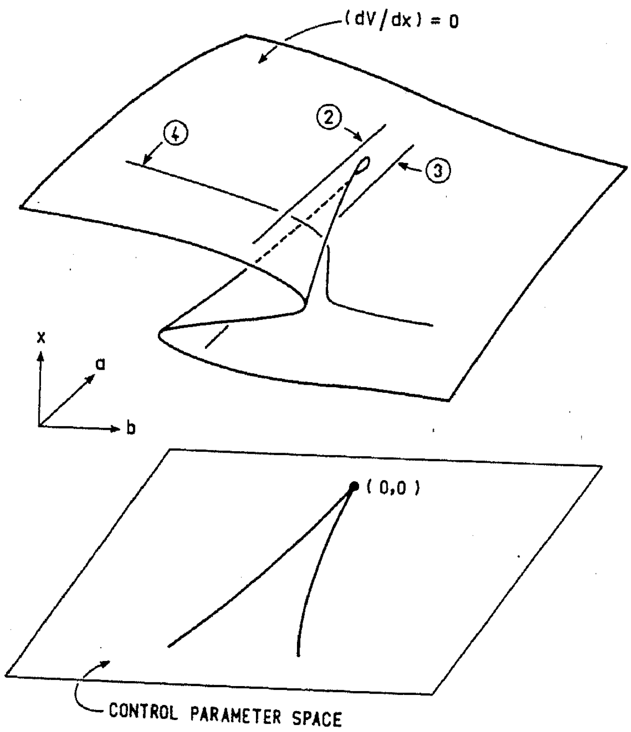

Figure 2. Critical manifold for the potential of (2). At the bottom is shown the projection of the fold lines in the a-b plane. Sketched on the manifold are a few trajectories. The system behaviour when driven along these trajectories is explained in the text and illustrated in figures 3 and 4.

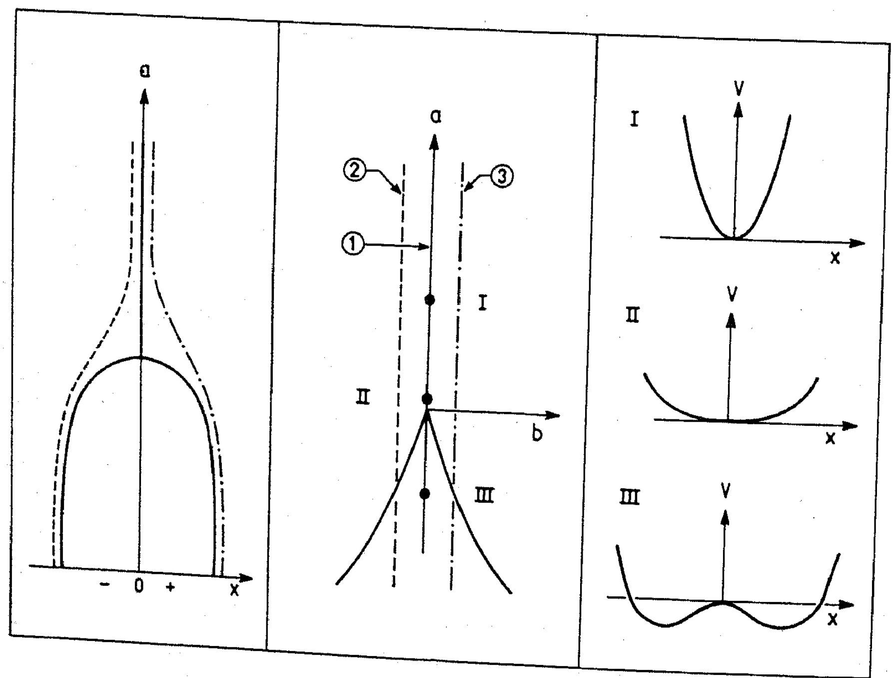

Figure 3. Shown at the centre is the cusp. On the right are sketched the forms of V corresponding to various points on the trajectory ①. On the left are sketched the order parameter variations for the three trajectories ①, ② and ③. For ① there is a bifurcation. The other two lead to a smooth behaviour without a phase transition.

the critical manifold (see also figure 2) and the system smoothly crosses over to one of the two folds representing a stable ordered state. Turning next to the trajectory ④ of figure 4 (see also figure 2), we note that it is orthogonal to those considered earlier. The changes in V as one moves along the trajectory are sketched and we observe that the system has two limiting behaviours in finding the appropriate minima. In one of these referred to as the delay convention (Gilmore 1981), the system remains in a stable or metastable state until that state disappears. The other case is referred to as Maxwell convention and is one where the system always hunts for the global minimum. If the system responds according to the delay convention, then there are overshoots as b is increased or decreased as a result of which a hysteresis occurs. In the Maxwell convention however, there is no hysteresis. In both cases the order parameter changes discontinuously at the transition.

The two conventions represent extremes in a continuum of possibilities, and which one is favoured depends essentially on the ratio of the noise N to the barrier height ΔE. If $(N/\Delta E) \ll 1$, the delay convention is respected whereas if $(N/\Delta E) \approx 1$ then noise promotes barrier jumps and helps the system to find the global minimum; in other words, the Maxwell convention is obeyed. The field-induced transition is usually

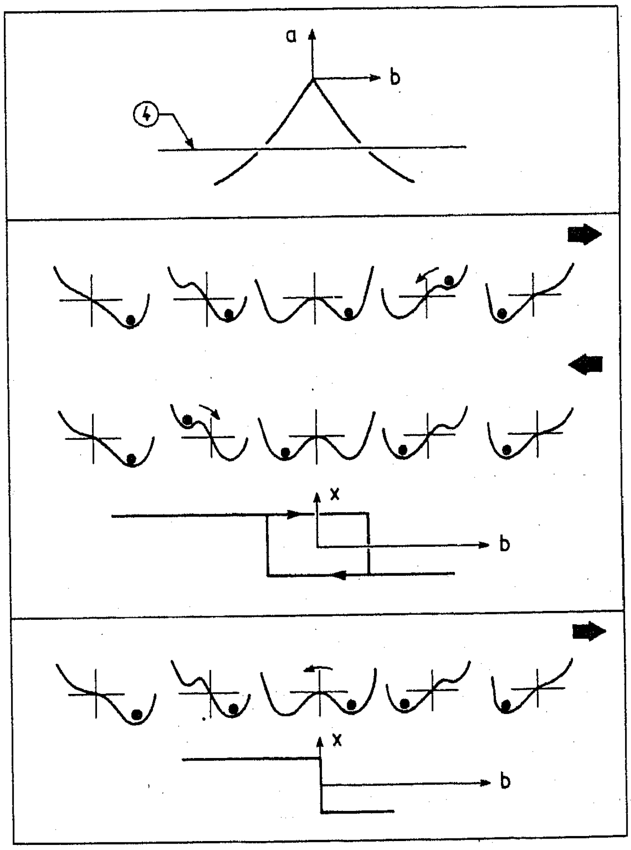

Figure 4. Illustration of system behaviour for the trajectory ④. When the system is driven back and forth along this trajectory, two scenarios are possible. In one, the system stays in the stable or metastable state till that state disappears. A hysteresis then appears as illustrated in the middle. This is the delay convention. However, if the system always chooses the global minimum, then there is no hysteresis as shown at the bottom. This is the Maxwell convention.

labelled as first order (see table 1) but Gilmore (1981) refers to the transition associated with the delay convention as being of zeroth order.

This concludes our survey, and we are now ready to examine the phase-transition behaviour of the amplifier.

3. Feedback amplifier

Consider the amplifier with positive feedback shown in figure 5a. Its effective gain is given by

$$A_{\text{eff}} \equiv |v_0/v_i| = A/(1 - A\beta), \tag{4}$$

Table 1. In the Ehrenfest classification scheme (Landau and Lifshitz 1959; Gilmore 1981), a phase transition is of order m at x_0 if $(\partial^i V/\partial x^i)_{x_0}$ is discontinuous for $i \geq m$ and continuous for $i < m$.

Order of the transition	Continuous functions	Discontinuous functions
0	—	$(V)_{x_0}$, $(\partial V/\partial x)_{x_0}$, etc
1	$(V)_{x_0}$	$(\partial V/\partial x)_{x_0}$, $(\partial^2 V/\partial x^2)_{x_0}$, etc
2	$(V)_{x_0}$, $(\partial V/\partial x)_{x_0}$	$(\partial^2 V/\partial x^2)_{x_0}$, $(\partial^3 V/\partial x^3)_{x_0}$, etc

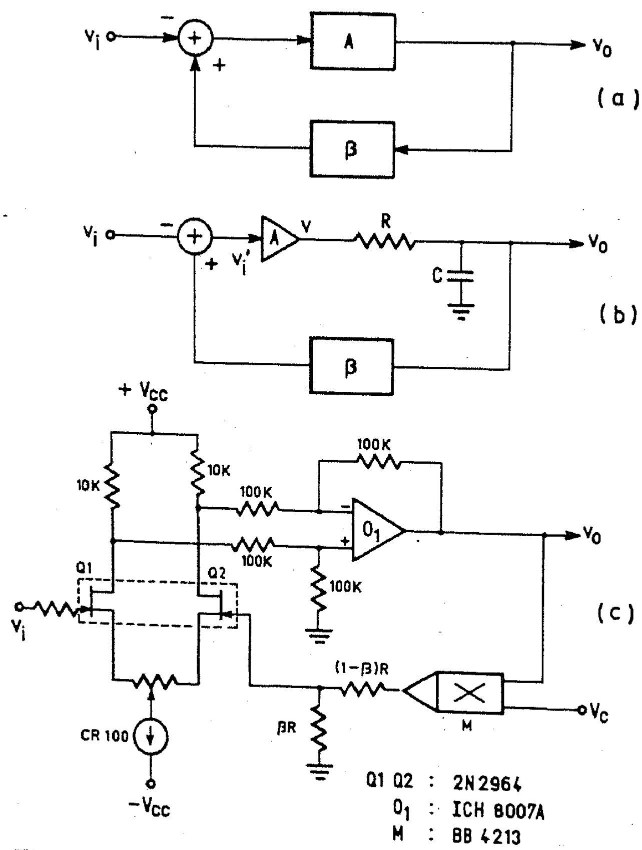

Figure 5. **a** and **b** are schematics of the feedback amplifier, with **b** showing explicitly the load capacitance C and load resistor R; **c** shows the circuit used by us.

where A is the gain without feedback, and β (>0) is the feedback factor. In figure 6 is sketched the transfer function (output *vs* input) for various β values. For experimental convenience, we have considered an amplifier whose output has a sign opposite to that of the input. If we set $v_i = 0$ and start from the condition $\beta = 0$, we see that the output voltage v_0 is also zero. As β is gradually increased, v_0 continues to remain zero until $A\beta > 1$. At this stage, the transfer function acquires the form sketched in figure 6c. Clearly two nonzero values for v_0 become possible even though $v_i = 0$, and the system randomly chooses one of these. Thus the appearance of a nonzero, steady output voltage even without an input is the equivalent of establishment of order (recall the spontaneous polarization in a ferromagnet below the Curie temperature), and clearly v_0 is the order parameter. As β increases further making $A\beta > 1$, v_0 also increases till it eventually saturates. The variation of v_0 with β is sketched in figure 6d and one sees a characteristic bifurcation pattern. Thus, even from a mere inspection of the transfer function characteristics, one is able to infer the existence of a transition akin to a second-order phase transition of equilibrium statistical mechanics. In passing, the similarity of the transfer function curves to the magnetization curves for an Ising magnet and the density *vs* chemical potential curves for a lattice gas is worth noting (Thomas 1968; Patashinskii and Pokrovski 1979).

We now probe the phase transition aspects in slightly greater depth for which purpose it is first necessary to consult figure 5b. Shown here is a more realistic representation of the amplifier in which is included the output impedance R and the load capacitance C. The actual output $v(t)$ is not accessible being internal to the circuit and we can measure only the apparent output $v_0(t)$. On account of nonlinearities, the

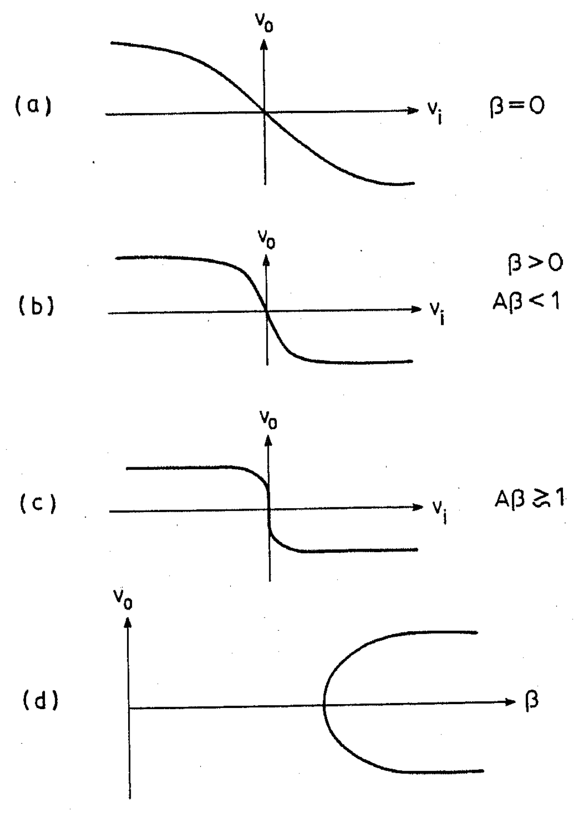

Figure 6. **a–c** schematically depict the transfer characteristics for various values of β. The resulting curve for output voltage v_0 *vs* β has the form in **d**. Compare with figure 1.

gain of the amplifier is in general a function of the net input voltage $v_i'(t)$ ($v_i' \equiv v_i - \beta v_0$), and for that reason may be written as $A(v_i')$. The actual circuit used by us is shown in figure 5c and will be explained shortly. For the present we merely note that the feedback β is derived from a resistive potential divider, and can be changed by varying the control voltage v_c.

Let us now compute the energy W involved in raising the output voltage to the value v_0, starting from an initial value of zero. This is the negative of the energy dissipated by the load resistor in the build up process. Thus

$$W = -R\int_0^\infty i^2(t)\mathrm{d}t = -C\int_0^{v_0} (v - v_0')\mathrm{d}v_0'$$

$$= \tfrac{1}{2}Cv_0^2 - C\int_0^{v_0} v\mathrm{d}v_0'.$$

Remembering $v = -A(v_i')v_i'$ and further that $v_i' = v_i - \beta v_0'$, the above result can be recast as

$$W = \tfrac{1}{2}Cv_0^2 + C\int_0^{v_0} (v_i - \beta v_0')A(v_i - \beta v_0')\mathrm{d}v_0'. \tag{5}$$

For the circuit used,

$$A(v_i') \approx A_0[1 - \alpha(v_i')^2], \tag{6}$$

where A_0 and α are constants. From (5) and (6) we obtain

$$W = C[(v_0^2/2)(1 - A\beta) + A\{v_0(v_i - \alpha v_i^3) + \tfrac{3}{2}\alpha\beta v_i^2 v_0^2 - \alpha\beta^2 v_i v_0^3 + \tfrac{1}{4}\alpha\beta^3 v_0^4\}], \tag{7}$$

which, for $v_i = 0$, reduces to

$$W = \frac{C}{2}(1 - A\beta)v_0^2 + (CA\alpha\beta^3/4)v_0^4, \tag{8}$$

having the familiar Landau form. It is not surprising therefore that the system exhibits a second-order phase transition with $v_i = 0$ and β as the control variable. We also note that the change of variable

$$x = (\beta v_0 - v_i) \tag{9}$$

leads to

$$W(x; a, b) = (a/2)x^2 + (x^4/4) + bx \tag{10}$$

with

$$a = (1 - A\beta)/(A\alpha\beta), \quad b = v_i/(A\alpha\beta). \tag{11}$$

We thus expect our amplifier to exhibit not only a second-order transition but indeed all the features related to the cusp catastrophe.

We turn again to figure 5c which gives the details of the circuit used by us. Here T_1 and T_2 are a matched pair of junction field-effect transistors (JFETS) connected as a differential amplifier with gain as given by (6) (Grey and Meyer 1977). The operational amplifier O_1 is used as a unity gain differential to a single-ended converter. The feedback system consists of an analog multiplier followed by a voltage divider network. The use of a multiplier allows for a continuous change in β by simply varying v_c. It may be added that for a given device, α is a fixed quantity. Thus, although it does contribute to the nonlinearity of the amplifier gain, α does not enjoy the status of a control parameter in our experiments; the phase transitions we observe are dictated only by v_c and β.

4. Experiments and results

We are now ready to discuss the experiments and the results obtained. Our first experiment was directed towards the verification of the bifurcation pattern of figure 6d. The experiment was performed by holding v_i at zero and sweeping β by connecting a ramp voltage to v_c. The resulting output voltage can be seen in figure 7a and the bifurcation is evident. In figure 7b are shown the output voltage fluctuations which, not surprisingly, are maximum at the transition (critical fluctuations). The bottom figure gives a combined presentation of the order parameter variation and the RMS value of the fluctuations. The divergence seen is the analog of the susceptibility divergence of condensed matter physics.

The above experiment was then repeated with $v_i \neq 0$ and given progressively larger values. The traces obtained are shown in figure 8a and are similar to the curves obtained for the temperature dependence of magnetization in the presence of an external magnetic field (Thomas 1968; Patashinskii and Pokrovski 1979). As one knows, there is

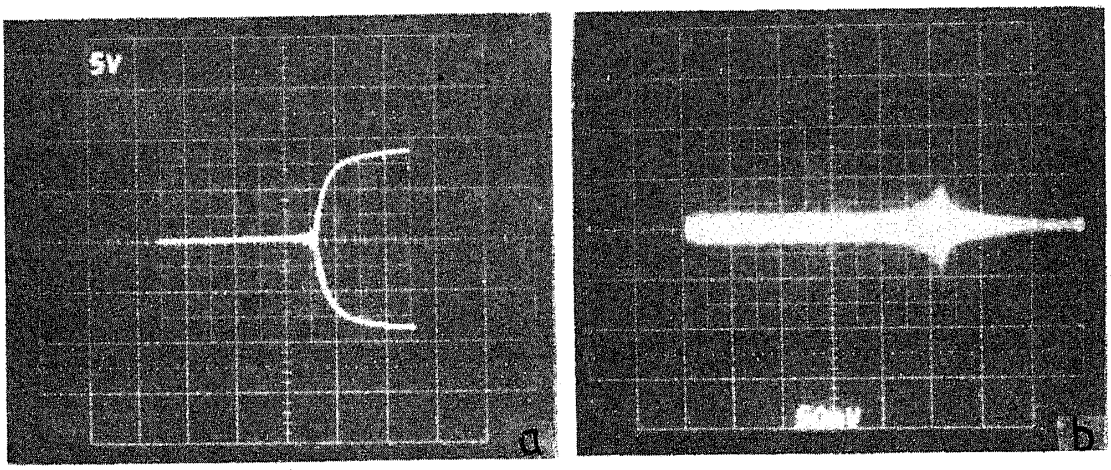

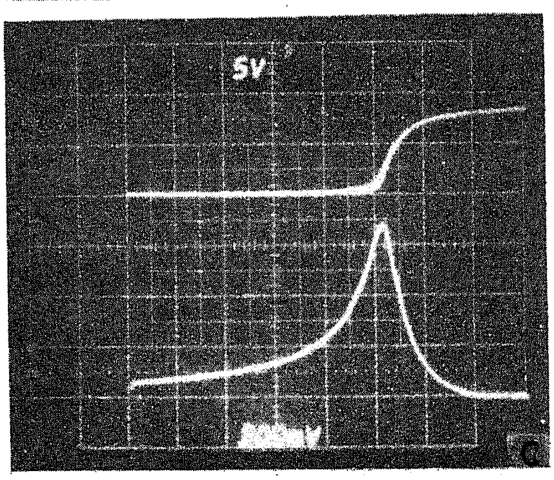

Figure 7. **a** shows the bifurcation observed with $v_i = 0$ and β varied. The accompanying noise fluctuations are shown in **b.** In **c** the order parameter variations can be seen along with the RMS value of the fluctuations.

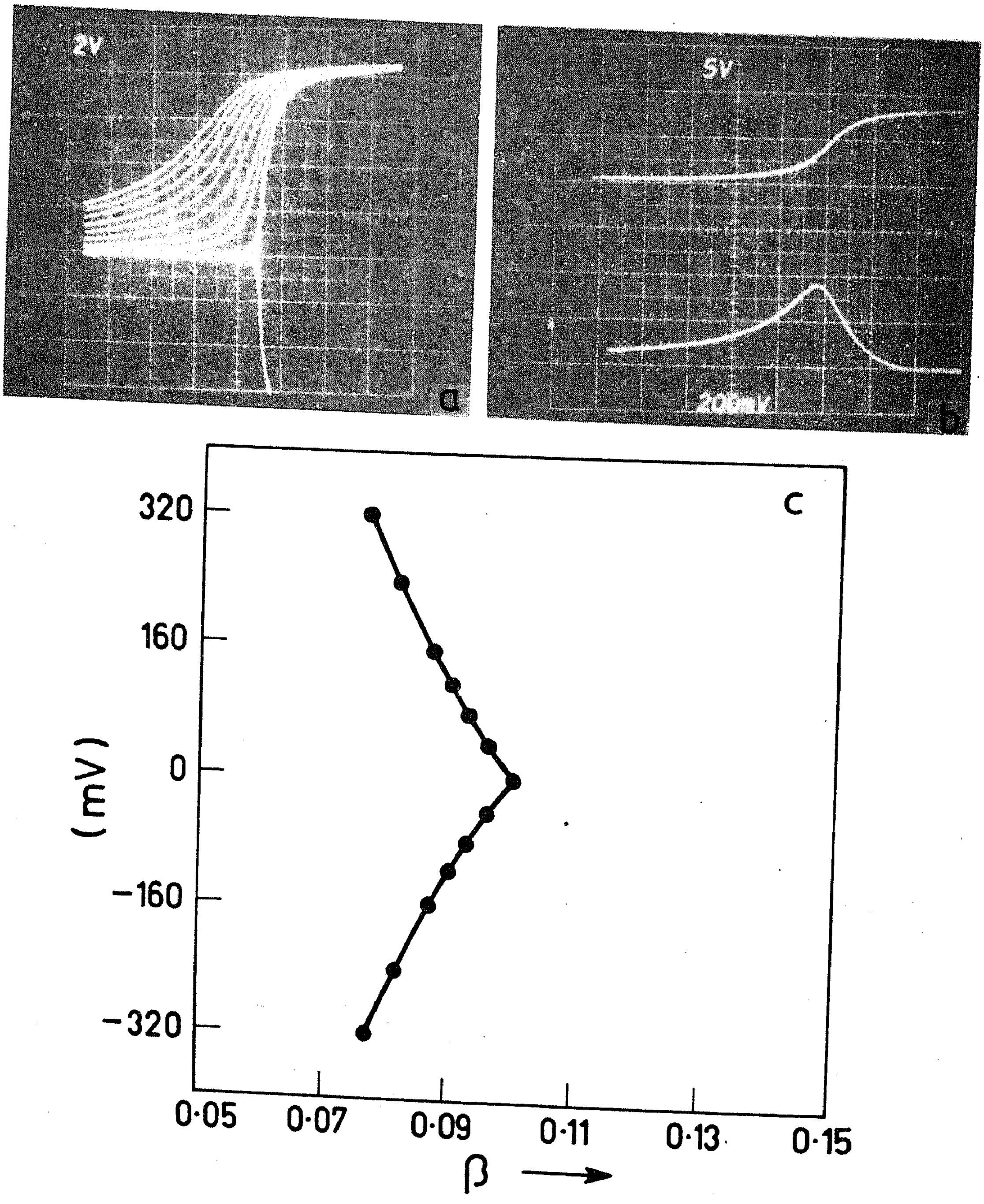

Figure 8. **a** shows the order parameter variation with β for various fixed values of v_i. Compare with left side of figure 3. In **b** is shown a typical order parameter curve and the concommitant RMS value of the fluctuations. A summary of the observed peak positions is shown in **c**. The solid lines are a guide to the eye.

no phase transition in this case (Patashinskii and Pokrovski 1979). This is also understandable if one examines the trajectories in figure 2 which are parallel to the a-axis and displaced from it. The system then smoothly rides over to one of the 'stable folds' without encountering a discontinuity. Another condensed matter example would be that of a fluid driven so as to miss the critical point (see, for example, figure 10.8 of Gilmore 1981).

Although there is no phase transition, we find that if the output voltage fluctuations are observed they show a peaking. Visual inspection suggests (see figure 8b) that the peak in the RMS value of the fluctuations occurs close to the point of inflection in the order parameter versus control parameter curve. In figure 8c we present a summary of the results on the peak positions. It is interesting in passing to note that such 'anomalous' fluctuations have been observed in several other experiments. For instance, Kabashima *et al* (1975) report a similar peak for the variance of the fluctuations accompanying the evolution of mean voltage during a transient in an electrical oscillator. Arecchi (1979) has drawn attention to similar phenomena in lasers. Suzuki (1979) has addressed himself to the theoretical aspects of this question but we have not probed that angle *vis-a-vis* our observations as that would require a separate and detailed set of experiments. We hope to carry out such investigations later.

We consider next experiments related to trajectory ④ of figure 4. As previously noted, whether or not hysteresis is observed depends on the convention obeyed. Figure 9a shows two traces obtained with β fixed and v_i varied. The conditions of the experiment were tailored for the delay convention to be operative and therefore a hysteresis is seen. However, the width of the loop was found to be dependent on $\dot{v}_i$. This dependence has been measured and is as in figure 9b.

Earlier we have discussed the role of noise in influencing the convention obeyed. To check this, we connected a noise source to the system and drove the system along the trajectory ④ with different noise inputs but $\dot{v}_i$ and β always remained the same. The results obtained are displayed in figure 10. With low noise a hysteresis is observed but when the noise level is increased it disappears as expected.

Figure 11 highlights in a comprehensive manner *via* three-dimensional plots, the various aspects currently under discussion. In figure 11a we have a computer plot of the critical manifold associated with the potential (2) while in 11b are presented the projections on the three orthogonal planes. Similar plots are given in figures 11c and 11d but with some difference. The manifold in 11c is a modification of that in 11a in that surgery has been done to the latter to remove the portions representing meta- and unstable regions. This 'surgered' manifold is the relevant one if Maxwell convention is followed. On the *a-b* plane this projects as line (instead of as a cusp), and transitions occur (without hysteresis) when this line is crossed. The projection on the *a-x* plane is the bifurcation curve and is the analog of the familiar coexistence curve of condensed matter physics. On the other hand, the critical manifold of figure 11a projects on the *a-x* plane as the spinodal. For comparison, we present in figures 11e and 11f, the (surgered) surface for a fluid and a ferromagnet (IFF Bulletin 1974).

We have already discussed the experimental study of the coexistence curve (see figure 8). To map the cusp and the spinodal, we observed the hysteresis loops for various β values. In obtaining these loops, the sweep rate was adjusted so that in terms of figure 9d we were close to the y-axis, thus minimizing the dependence of the results on the sweep rates. The cusp and the spinodal could be readily constructed from the width and the height of the hysteresis loops, and are shown in figures 12 and 13. Note that we have used the $(v_0; \beta, v_i)$ representation instead of the $(x; a, b)$ representation but the results are equivalent, and the expected forms do appear without too much distortion. In fact, the spinodal is given by $v_s = (v_0/\sqrt{3})$. This is the so-called 'root-three rule' well-known to metallurgists (de Fontaine 1979).

We have also investigated the noise aspects of zero and first-order transitions. This was done by varying the system time constant τ_s and studying the system response when

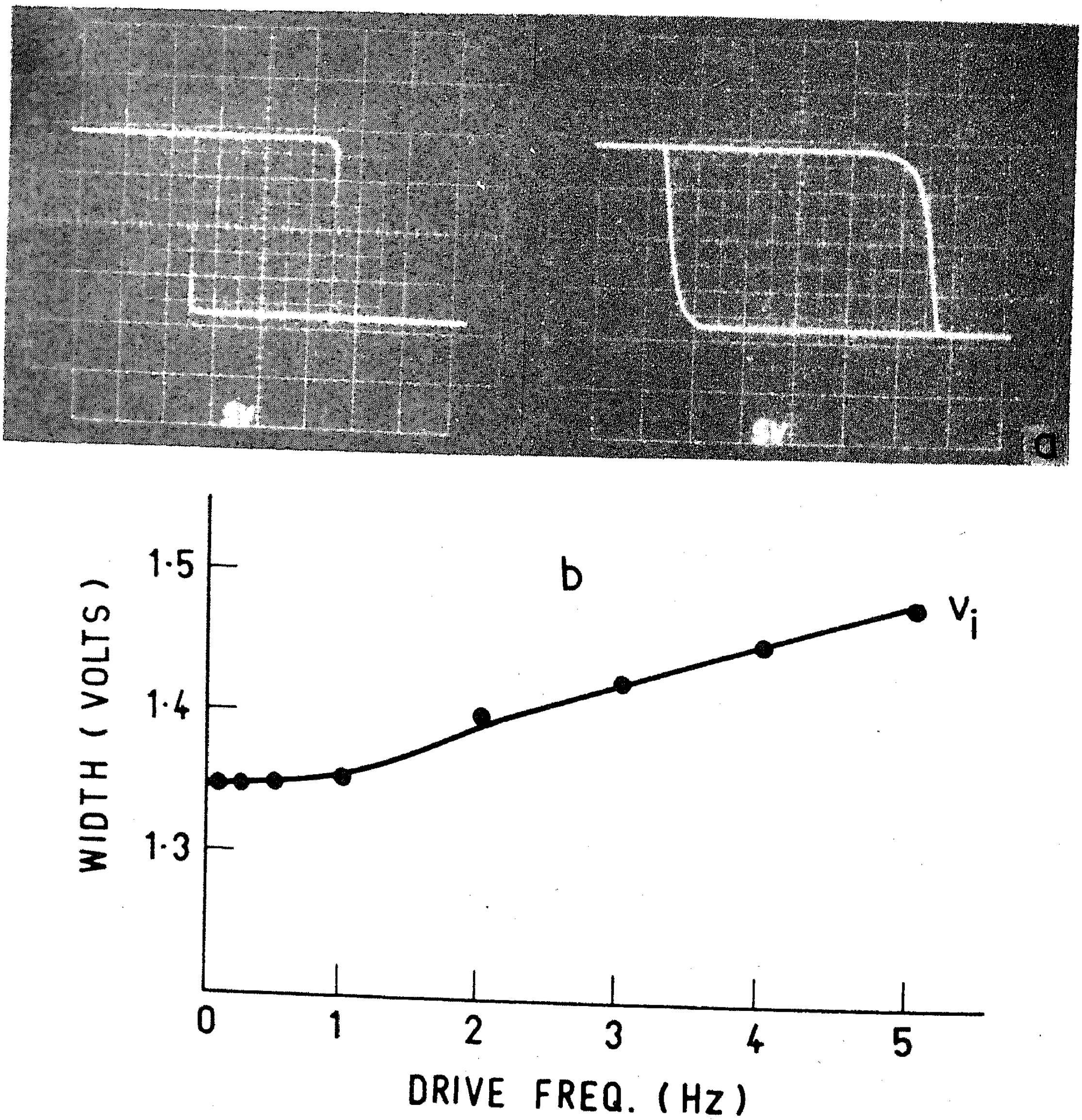

Figure 9. **a** Hysteresis loops corresponding to the *same* trajectory (type ④) but obtained with different $\dot{v}_i$. The widths depend on $\dot{v}_i$. This dependence has been measured and is as in **b**.

driven along trajectory ④, with the other conditions (*i.e.*, β, $\dot{v}_i$) remaining the same. Typical results are given in figure 14. The hysteresis loops observed are the same (the oscilloscope sweep rate was much lower than $\dot{v}_i$) but the magnitude of fluctuations observed at cross-over differs. The fluctuations are barely in evidence where τ_s is small but are significant when τ_s is large.

There is a simple way of understanding these results. In undergoing the transition, the (observed) voltage swings from $-v_{sat}$ to $+v_{sat}$ (or vice versa depending on the initial state). At this stage effective input v_i' essentially consists of the noise in v_i since $\langle v_i' \rangle$ is zero around then. Since $A \gg 1$, the (true) output v (see figure 5b) quickly saturates and swings between $\pm v_{sat}$, with zero crossings of v matching those of the noise in v_i'. In other words, in the neighbourhood of the cross-over, $v(t)$ is essentially a random telegraph signal (Davenport and Root 1958) of amplitude $\pm v_{sat}$. However, on account

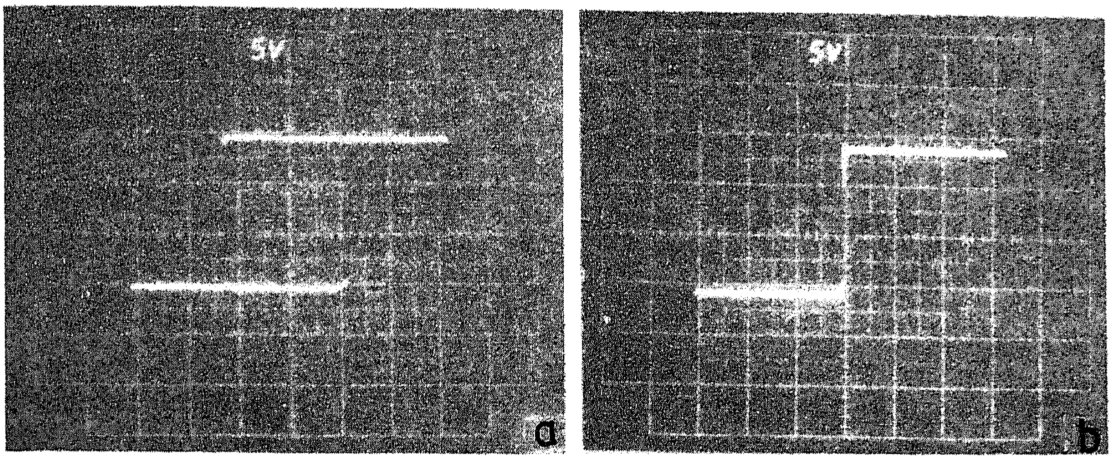

Figure 10. Role of noise in influencing the convention obeyed. If noise is low, the delay convention is obeyed and a hysteresis is seen (left). If the noise is large, Maxwell convention is obeyed and no hysteresis is seen (right).

of the system time constant, the voltage that one actually observes namely v_0, has a modified character. Until $\langle v_0 \rangle$ builds up to a sufficient value and is able to feedback a significant voltage to O_1, the fluctuations in v_i' have a controlling say. The time evolution of v_0 in the region of cross-over may thus be understood by considering the equation

$$RC\frac{dv_0}{dt} + v_0 = f(t), \tag{12}$$

where $f(t)$ is the random telegraph output having the value (say) $+v_{sat}$ at $t = 0$, and switching (randomly) at time $t_1, t_2 \ldots$ etc. From (12) we have

$$v_0(t_1) = 2v_{sat}[1 - \exp(-t_1/RC)] - v_{sat}$$
$$v_0(t_2) = v_0(t_1) - [v_0(t_1) + v_{sat}][1 - \exp\{(t_1 - t_2)/RC\}] \ldots \tag{13}$$

If $\langle \Delta t_i \rangle / RC \ll 1$, v_0 will quickly saturate and fluctuations in v_0 will not be seen. The opposite will be true if $\langle \Delta t_i \rangle / RC \gg 1$. Remembering that RC is related to τ_s and noting further that $\langle \Delta t_i \rangle$ is related to τ_c, the correlation time of the output noise (Jakeman 1970), we find that fluctuations occur if $\tau_s \gg \tau_c$ and not otherwise. Similar results were obtained for the case when Maxwell convention was obeyed.

In condensed matter physics, quench experiments are quite common. For example, one often supercools or superheats a system and observes the subsequent evolution towards equilibrium. As far as temperature quenches are concerned, it is well-known that the region of the phase diagram within the coexistence curve can be divided into a region of instability and a region of metastability. The former is the region between the spinodal and the coexistence curve. In a computer simulation of the kinetics of the Ising ferromagnet, Lebowitz *et al* (1982) have observed wide variation in the relaxation times even though the system was quenched to the same temperature. This variation was related to the location of the terminal point, in particular on whether it was in the unstable or metastable region (see the points 1–5 in figure 1 of Lebowitz *et al* (1982) and also the corresponding relaxation curves given in their figure 4).

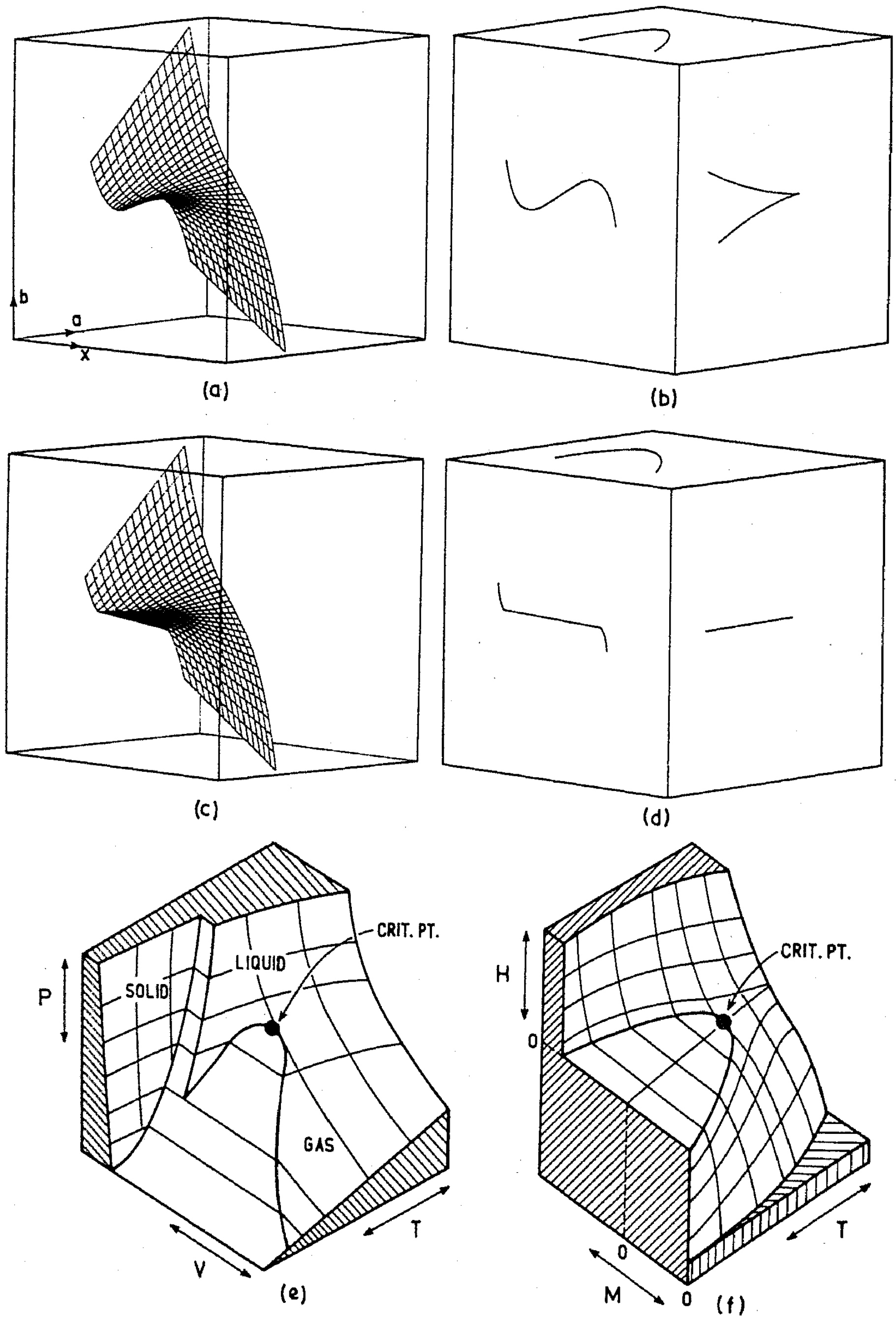

Figure 11. **a** shows a computer plot of the critical manifold associated with potential (2). The manifold is enclosed in a box with planes parallel to the *x-a*, *a-b* and *x-b* planes; **b** shows the projections of the critical manifold on the three planes. On the *x-a* plane it is a spinodal, on the *a-b* plane a cusp and on the *x-b* plane a *S*; **c** and **d** are corresponding figures for the surfaced manifold while **e** and **f** (after IFF Bulletin) are representative examples from condensed matter.

We have carried out similar quench experiments by suitably controlling the parameter β. The results may be summarized as follows: Considering figure 13, a β-quench drives the system along a vertical line, and our interest is in the situation when the terminal point is in the shaded region. This being an unstable domain, the system relaxes to a stable state, for which there are two possibilities defined by the intersection

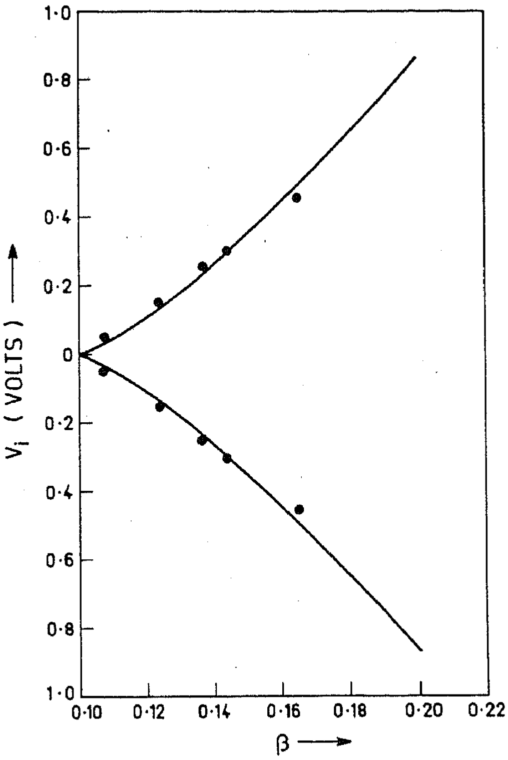

Figure 12. Observed and calculated cusp lines.

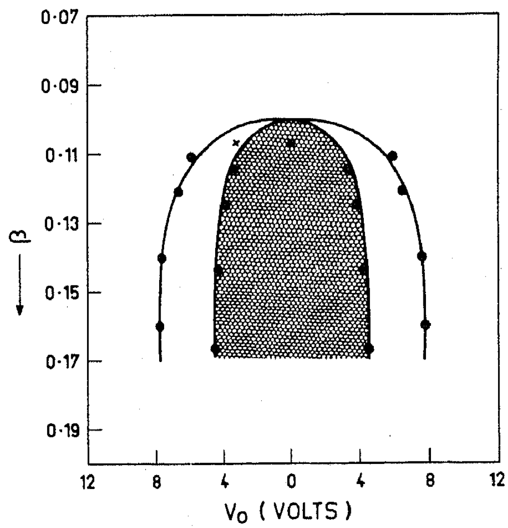

Figure 13. Observed and computed bifurcation and spinodal lines. The shaded region represents instability, while the region between the spinodal and the bifurcation line represents metastability. The crosses denote terminal points of the β quench experiments.

of the coexistence curve with the horizontal corresponding to the final β value. If $v_i = 0$, there is equal probability of the two stable states being realized. However, if $v_i \neq 0$, then the vertical quench line is on one side of the line $v_0 = 0$, and the closer of the two stable states get preferred. The voltage step associated with the relaxation corresponds to the difference $|v_0 \text{ (initial)} - v_0 \text{ (final)}|$.

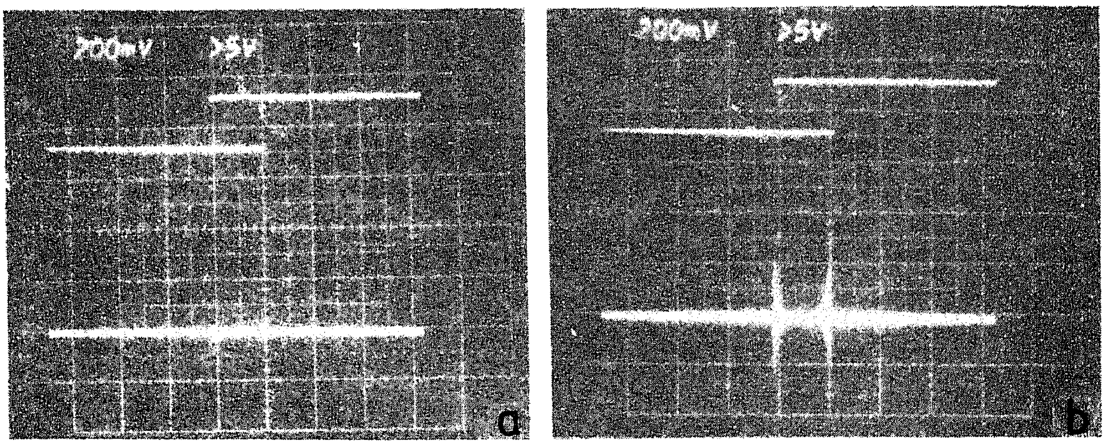

Figure 14. Noise in zero-order transitions. If $\tau_s \ll \tau_c$, critical fluctuations are barely in evidence (left). For $\tau_s \gg \tau_c$, they are prominent (right).

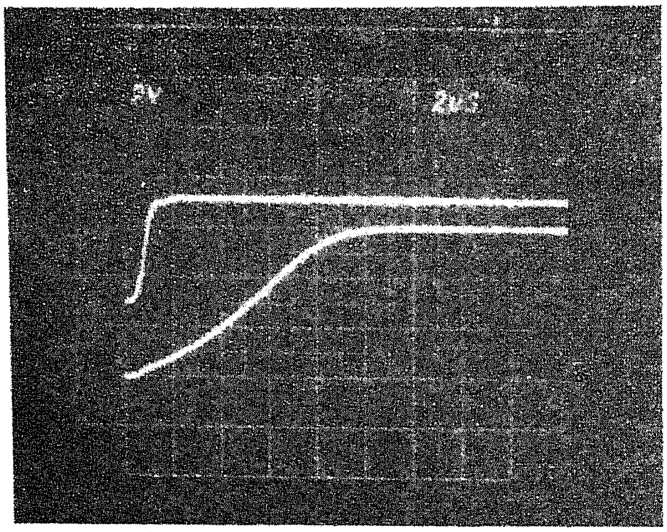

Figure 15. Results of β-quench experiments analogous to the temperature quench experiments of Lebowitz *et al* (1982). The terminal points of the quench are shown in figure 13. A quench into the metastable region produces a slow relaxation while a quench into the unstable region produces a fast relaxation.

Typical quench results are shown in figure 15, with the corresponding terminal points being as indicated in figure 13. Like Lebowitz *et al* (1982), we too observe a marked variation in the relaxation times. In general, the relaxation time becomes longer as the terminal point gets closer the 'stable' point (on the coexistence curve).

Besides temperature quenches, (isothermal) field quenches are also known, and Billotet and Binder (1979) for example, discuss them (see their figure 1). In such experiments, the system to start with is in one of the two possible ordered states; also the field is zero. In terms of the critical manifold (figure 2), this implies that x lies on one of the stable sheets, the top one say. Since the field is zero, x will actually lie on the line of intersection of the top fold with the plane $b = 0$. Suppose we now apply a field Δb with a sign such that it tips the system towards the edge of the fold and facilitates its 'rolling'

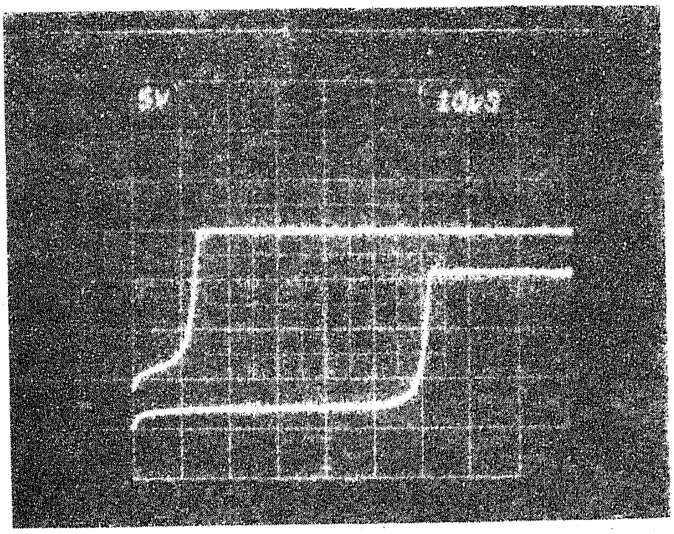

Figure 16. Results of the field-quench experiments analogous to those discussed by Billotet and Binder (1979). Deep quenches produce rapid relaxation but if the quench is shallow, the system is trapped for a while in a metastable state.

over. The relaxation time associated with such a phase change depends on the depth of the quench *i.e.* on the magnitude of Δb. Billotet and Binder (1979) have studied such relaxation within the framework of the Ginzburg-Landau theory and have shown that if Δb is large, then the system rapidly relaxes. However, if Δb is small, then the system becomes trapped in a metastable state for a while before finally crossing over. This trapping leads to a plateau in the relaxation curve. Our experiments (β fixed and v_i quenched from zero to Δv_i) reveal similar trends as may be seen from figure 16. In fact the similarity of our results to figure 1 of Billotet and Binder is quite striking.

We thus see that the analogy in the behavioural pattern of the feedback amplifier to phase transitions of condensed matter applies not only to the ordering aspects but extends also to kinetics.

5. Summary and conclusions

In this paper we have presented detailed experimental results on the (nonequilibrium) phase transition aspects of the feedback amplifier. By recognizing that the relevant potential has the Landau form, it has been possible to map the behaviour to that expected for the cusp catastrophe. Various features related to the critical manifold have been explored by driving the system along suitable trajectories in control parameter space, and we have demonstrated second, first and zero-order transitions. By a detailed study of the hysteresis patterns, the cusp and the spinodal have been mapped. In addition, the gradual 'cross-over' (*i.e.* without a phase transition) in the presence of an external 'field' has also been studied. Incidentally, since β and v_i can both be varied independently and simultaneously, it is possible to explore various trajectories other than those studied by us like, for example, the curved trajectories considered by Gilmore (1981) in his figure 15.9.

Besides studies related to the mean value of the order parameter, we have also observed the order parameter fluctuations and shown that they become large near the second-order phase transition. In field-induced transitions, we find that the magnitude of the critical fluctuations depends on the ratio of the system response time τ_s to the correlation time τ_c for the noise. We have also observed that while for some patterns of control parameter variation (*i.e.* along trajectories 2 and 3) no phase transition occurs, the fluctuations do become large at some point during the variation of the control parameter. In addition, quench experiments analogous to those familiar in condensed matter physics have been performed, and with similar results.

We have not measured exponents but, based on our other observations, we do not expect anything other than mean-field values. For pedagogic completeness we have drawn attention wherever necessary, to appropriate analogies from condensed matter physics. We also remark that since the experiments reported are quite easy to perform, they could well form a useful tutorial aid to students wanting to become familiar with various concepts relating to phase transitions. Lastly we observe that extensions are also possible to our system to study the analogues of the interesting problems which occur in quantum optics (Arrechi 1979; Bonifacio and Lugiato 1979).

Acknowledgements

One of the authors (GV) thanks V Balakrishnan for discussions and S R Shenoy for correspondence regarding spinodals. They are also grateful to K Anantharaman for help with computer graphics, and to the referees for their comments.

References

Arecchi F T 1979 in *Pattern formation by dynamic systems and pattern recognition* (Ed) H Haken (Berlin: Springer Verlag) p 28
Billotet C and Binder K 1979 *Z. Phys.* **B32** 195
Bonifacio R and Lugiato L A 1979 in *Pattern formation by dynamic systems and pattern recognition* (Ed) H Haken (Berlin: Springer Verlag) p 16
Davenport W B and Root W L 1958 *An introduction to the theory of random signals and noise* (New York: McGraw Hill)
de Fontaine D 1979 *Solid State Phys.* **34** 73
Eigen M 1971 *Naturwissenschaften* **33a** 465
Gilmore R 1981 *Catastrophe theory for scientists and engineers* (New York: John Wiley)
Glansdorf P and Prigogine I 1971 *Thermodynamic theory of structure, stability and fluctuations* (New York: Wiley)
Grey P R and Meyer R G 1977 *Analysis and design of analog integrated circuits* (New York: Wiley)
Haken H 1978 *Synergetics—An introduction* (Berlin: Springer Verlag)
Horn P M, Carruthers T and Long M T 1976 *Phys. Rev.* **A34** 833
IFF Bulletin 1974 (Julich: IFF)
Jakeman E 1970 *J. Phys.* **A3** 201
Kabashima S, Itsumi M, Kawakubo T and Nagashima T 1975 *J. Phys. Soc. Jpn.* **39** 1183
Kabashima S, Kogure S, Kawakubo T and Okade T 1979 *J. Appl. Phys.* **50** 6296
Kabashima S, Yamazaki H and Kawakubo T 1976 *J. Phys. Soc. Jpn.* **40** 921
Kawakubo T and Kabashima S 1974 *J. Phys. Soc. Jpn.* **37** 1199
Keizer J 1981 *J. Chem. Phys.* **74** 1350
Landau L D and Lifshitz E M 1959 *Statistical physics* (Oxford: Pergamon Press)
Landauer R 1962 *J. Appl. Phys.* **33** 2209
Lebowitz J L, Marro J and Kalos M H 1982 *Acta Metall.* **30** 297
Neelakantan K and Venkataraman G 1982 *Acta Metall.* **31** 77

Nicolis G 1980 in *Systems far from equilibrium* (Ed) L Garrido (Berlin: Springer Verlag) p 91
Nicolis G and Prigogine I 1977 *Self organization in nonequilibrium systems* (New York: Wiley)
Pacault A and Vidal C (Eds) 1979 *Synergetics* (Berlin: Springer Verlag)
Patashinskii A Z and Pokrovski V I 1979 *Fluctuation theory of phase transitions* (Oxford: Pergamon Press)
Prigogine I and Nicolis G 1971 *Q. Rev. Biophys.* **4** 107
Shenoy S R and Agarwal G S 1981 *Phys. Rev.* **B23** 1977
Suzuki M 1979 in *Synergetics* (Eds) A Pacault and C Vidal (Berlin: Springer Verlag) p 94
Swinney H L and Gollub J P 1981 *Hydrodynamic instabilities and the transition to turbulence* (Berlin: Springer Verlag)
Venkataraman G 1979 *Trans. Indian Inst. Metals* **32** 435
Venkataraman G and Balakrishnan V 1978 *Phys. News* **2** 1
Thomas H 1968 in *Theory of condensed matter* (Vienna: IAEA) p 357